# Complex refractive index of limestone in the visible and infrared

Marvin R. Querry, Gordon Osborne, Ken Lies, Ray Jordon, and Raymond M. Coveney, Jr.

Near normal-incidence relative spectular reflectance was measured throughout the 0.2–32.8-$\mu$m wavelength region for three cut and polished samples of Bethany Falls limestone. Water, for which the complex refractive index is well known, was the reflectance standard. Although the visual appearances of the three samples were quite different, the relative reflectance spectra for the three samples were nearly identical. The three relative reflectance spectra were averaged to obtain a composite relative reflectance spectrum. Kramers-Kronig analysis of the composite relative reflectance spectrum then provided spectral values of the complex refractive index for limestone. A classical Lorentz dispersion analysis was also made of the composite relative reflectance spectrum, and the resulting dispersion parameters were tabulated. Infrared bands characteristic of the carbonate ion $CO_3^{-2}$ of the calcite comprising the limestone appeared as strong features in the spectra.

## I. Introduction

The advent of remote sensing by use of optical instruments mounted in aircraft and satellites, and an interest in the thermal budget of the planets, have produced an increasing interest in spectral values of the complex refractive index $N(\lambda) = n(\lambda) + ik(\lambda)$ of materials commonly found on terrestial and other planetary surfaces. The present investigation was undertaken to obtain spectral values of $N(\lambda)_l$ for limestone which consists primarily of randomly oriented microcrystals of calcite. Other constituents of limestone are randomly oriented microcrystals of dolomite and organic fossil material. Limestone is relatively abundant in the terrestial environment, but would be on other planetary surfaces only if biological conditions as we know them on earth once existed on those planets.

In the present investigation spectral values $N(\lambda)_l$ are obtained in the following manner. First the near-normal incidence relative reflectance $R(\lambda) = R(\lambda)_l/R(\lambda)_w$ of limestone $l$, with water $w$ as the reflectance standard, was measured throughout the 0.2–32.8-$\mu$m wavelength region. Second, a Kramers-Kronig phase-shift dispersion analysis[1,2] of $R(\lambda)$ provided a spectrum $\Delta\phi(\lambda)$ which is the difference in phase change for electromagnetic waves of wavelength $\lambda$ reflected from the limestone and from the water standard. An algorithm[1,2] that uses $R(\lambda)$, $\Delta\phi(\lambda)$, and measured angle of incidence $\theta$, and known spectral values for the complex refractive index $N(\lambda)_w$ of water then provided spectral values of $N(\lambda)_l$. Additionally, a classical Lorentz dispersion analysis of the absolute reflectance spectrum $R(\lambda)_l$ of limestone yielded spectral values of the complex dielectric function $\epsilon(\lambda)_l$ from which $N(\lambda)_l$ were readily obtained.

The optical properties of natural minerals and rocks have been investigated by several other scientists. Aronson and Strong[3] obtained Lorentz parameters in the ir for muscovite mica, anorthosite, diopsidic pyroxenite, almandite-pyrope, garnet, and soda lime glass. Pollack *et al.*[4] obtained Lorentz parameters for obsidian, basaltic glass, basalt, and andesite. Spitzer and Kleinman[5] obtained Lorentz parameters for the ir lattice bands of quartz. Holland *et al.*[6] measured ir reflectance spectra in the 2–50-$\mu$m wavelength region and computed $N(\lambda)$ by use of Kramers-Kronig techniques for quartz, calcite, dolomite, fluorite, galena, sphalerite, brucite, magnetite, goethite, and hematite. Analysis of the optical properties of minerals and rocks in the visible and ir are also provided by Refs. 7–10.

## II. Preparation of Samples

Three samples of the Bethany Falls limestone, a prominent member of the Swope formation,[11] were collected from the approximate center of Section 7-R32W-T49N in northeast Kansas City, Missouri. All samples were prepared by standard polishing techniques. Following a final buffing with 0.1-$\mu$m Linde B, the samples were examined for scratches and pits by use of a Vickers metalore microscope. The three polished

All authors are at University of Missouri-Kansas City, Kansas City, Missouri 64110; R. M. Coveney is with the Geosciences Department; the others are with the Physics Department.

Received 31 May 1977.
0003-6935/78/0201-0353$0.50/0.

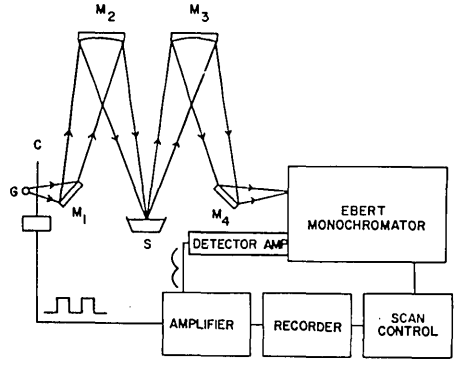


Fig. 1. A block diagram of the reflectometer system (see Sec. III for complete details).

limestone samples were slightly marred by pits and cracks due to the presence of natural vugs and joints. Modal analyses were performed by point counting in order to assess the impact of the pits and cracks on subsequent reflectance spectra. Modal analyses revealed 2.96–7.89 aerial % cavities with a mean aerial % of 4.60. Although scattering losses are a function of wavelength, the reflectance spectra described hereinafter were increased by a factor of 1.04 to compensate for the presence of the pits and cracks which were random in size and orientation.

The Bethany Falls samples consisted of dense fine-grained buff to gray mottled limestone. Calcite constituted greater than 99.7% of the samples, the remainder was sparse pyrite. Because the Bethany Falls limestone commonly contained dolomite in abundance, this mineral was specifically searched for. However, results from both stained thin sections and x-ray diffraction disclosed no dolomite.

Texturally the samples were all very similar, typically containing 5–20-$\mu$m irregular interlocking grains and no readily apparent preferred orientation. Some grains were as small as 2 $\mu$m, and others were rare and widely dispersed clots of exceptionally large 40–200-$\mu$m grains which appeared to be fossil fragments. A minor, but ubiquitous, dusting of 2-$\mu$m diam pyrite grains was also present. Modal analysis of polished sections disclosed from 0.14% to 0.2% pyrite.

## III. Acquisition of Reflectance Spectra

A block diagram of the reflectometer system is shown in Fig. 1. Radiant flux from a glower $G$ was chopped at $C$ and was then focused by an $f/5$ optical system, consisting of plane mirror $M_1$ and spherical mirror $M_2$, on the upper surface of the sample $S$. The angle of incidence $\theta$ was 6.2° for the central ray from $M_2$ incident on the upper surface of $S$. Radiant flux reflected from $S$ was imaged by an identical optical system ($M_3$ and $M_4$) on the entrance slit of a Perkin-Elmer Ebert double-pass grating monochromator. The spectral width of the exit slits $\Delta\lambda$ was adjusted manually to assure spectral resolution $\lambda/\Delta\lambda$ of 100 or greater. At the exit slit of the monochromator the radiant flux was optically filtered to remove higher diffraction orders and was then focused on a thermopile detector equipped with a CsI window. In the visible and near ir regions the source $G$ was a tungsten lamp, and in the uv it was a deuterium lamp. The detectors in the uv-visible and near-ir regions were photomultiplier tubes and PbS, respectively. The signal from the detector was processed by a lockin amplifier. The analog output from the lockin was applied to the input of a stripchart recorder. Data were manually read from the stripcharts and then punched on computer cards.

In the present investigation we measured relative reflectance $R(\lambda) = R(\lambda)_l/R(\lambda)_w$, where $l$ and $w$ denote limestone and water, respectively. Data were acquired in the following order: $Z$-$W$-$L$-$W$-$L$-$W$-$L$-$W$-$Z$, where $Z$ indicates a spectral scan made when the beam of radiant flex was blocked just in front of the source $G$, $W$ indicates a spectral scan made with the water standard $w$ in the sample position, and each $L$ indicates a sequence of three scans, one for each of the three limestone samples. After data were acquired throughout the 0.2–32.8-$\mu$m spectral region the relative reflectance of the limestone samples was calculated as follows. First, the average of the two spectral scans $Z$ was subtracted point by point from the other thirteen spectral scans denoted by $W$ and $L$. Second, the three spectral scans denoted by each $L$ were averaged and ratioed to the average of the spectral scans $W$ made just before and after spectral scans $L$. This procedure provided three relative reflectance spectra, one for each of the three groups of three spectral scans $L$, which were then averaged to provide a composite spectrum and standard deviations. The composite spectrum was then multiplied by 1.04 as indicated in Sec. II. The absolute reflectance $R(\lambda)_l$ of the limestone was provided by $R(\lambda)_l = R(\lambda)R(\lambda)_w$, where $R(\lambda)_w$ was computed by use of the Fresnel equations and known values[12] for $N(\lambda)_w$, and $R(\lambda)$ designates the composite relative reflectance spectrum. The absolute reflectance spectrum $R(\lambda)_l$ of limestone is shown in Figs. 2 and 3. The standard deviations were $\pm 0.06R(\lambda)_l$ in the spectral region beyond 25 $\mu$m and reduced to about $\pm 0.01R(\lambda)_l$ in the spectral region from 0.2 $\mu$m to 20 $\mu$m.

Evidence of birefringence was not observed as the limestone samples were rotated while placed in the reflectometer; thus we treat limestone as a homogeneous isotropic material.

## IV. Complex Refractive Index $N(\lambda)_l$

Spectral values of the complex refractive index $N(\lambda)_l$ were obtained by use of the Kramers-Kronig algorithm described in Refs. 1 and 2. Values for $N(\lambda)_l$ obtained in this manner appear in graphical form in Figs. 4 and 5. Evaluation of the Kramers-Kronig dispersion relation requires an integration of $R(\lambda)$ over the entire electromagnetic spectrum. Our data, however, extended only from 0.2 $\mu$m to 32.8 $\mu$m. Thus we made the approximations that $R(\lambda) = R(0.2\ \mu\text{m})$ throughout the $0 \leq \lambda \leq 0.2$-$\mu$m region and $R(\lambda) = R(32.8\ \mu\text{m})$ throughout the $32.8 \leq \lambda \leq \infty$ $\mu$m region. The latter

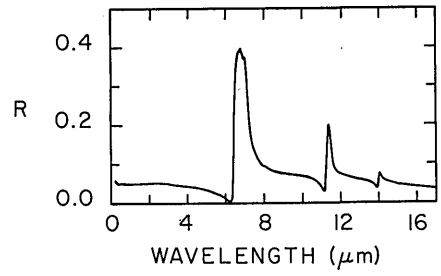


Fig. 2. Near-normal incidence composite absolute reflectance spectrum $R(\lambda)_l$ for Bethany Falls limestone in the wavelength region from 0.2 μm to 17 μm.

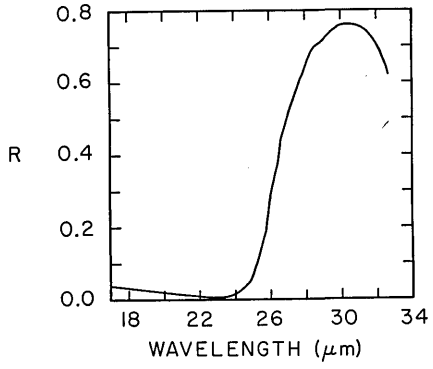


Fig. 3. Near-normal incidence composite absolute reflectance spectrum $R(\lambda)_l$ for Bethany Falls limestone in the wavelength region from 17 μm to 32.8 μm.

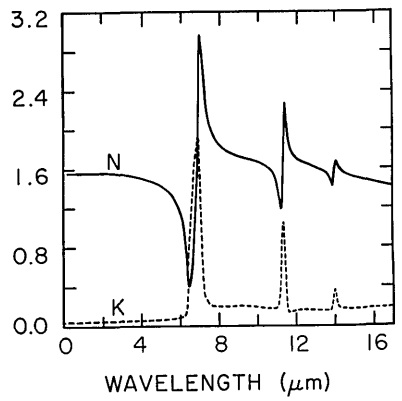


Fig. 4. Complex refractive index $N(\lambda)_l = n(\lambda)_l + ik(\lambda)_l$ in the wavelength region from 0.2 μm to 17 μm as obtained from Kramers-Kronig analysis of the near-normal incidence composite relative reflectance spectrum $R(\lambda) = R(\lambda)_l/R(\lambda)_w$.

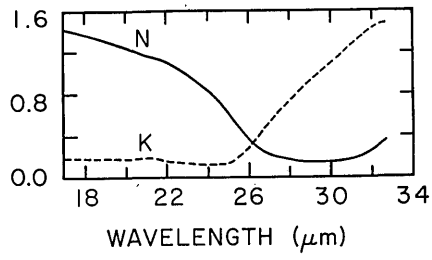


Fig. 5. Complex refractive index $N(\lambda)_l = n(\lambda)_l + ik(\lambda)_l$ in the wavelength region from 17 μm to 32.8 μm as obtained from Kramers-Kronig analysis of the near-normal incidence composite relative reflectance spectrum $R(\lambda) = R(\lambda)_l/R(\lambda)_w$.

assumption is open to serious inquiry because calcite, the primary constituent of limestone, possesses other ir active lattice bands at wavelengths greater than 32.8 μm.

Spectral values of $N(\lambda)_l$ were also obtained by use of classical Lorentz dispersion theory. According to the Lorentz theory the complex dielectric function $\epsilon(\nu)$ at wavenumber $\nu = \lambda^{-1}$ is given by

$$\epsilon(\nu) = \epsilon_\infty + \sum_j \frac{4\pi\rho_j\nu_j{}^2[(\nu_j{}^2 - \nu^2) + i\gamma_j\nu_j\nu]}{(\nu_j{}^2 - \nu^2)^2 + (\gamma_j\nu_j\nu)^2}, \quad (1)$$

where $\epsilon_\infty$ is the high frequency dielectric constant, $\rho_j$ is the strength of the $j$th ir active band, $\nu_j = \lambda_j{}^{-1}$ is the central wavenumber position of the $j$th ir active band, and $\gamma_j$ is a damping coefficient. Lorentz parameters determined for limestone appear in Table I. The relation between $N(\lambda)_l$ and $\epsilon(\lambda)_l$ is

$$\epsilon(\lambda)_l = N(\lambda)_l{}^2, \quad (2)$$

from which the real and imaginary parts of $N(\lambda)_l = n(\lambda)_l + ik(\lambda)_l$ can be determined.

A comparison of values for $N(\lambda)_l$ obtained by Kramers-Kronig techniques and by use of the Lorentz theory showed reasonable agreement in the spectral region from 0.2 μm to about 25 μm and increasingly poor agreement as wavelength increased beyond 25 μm. Both the real $n(\lambda)_l$ and imaginary $k(\lambda)_l$ parts of $N(\lambda)_l$ were higher in the 25–32.8-μm region for the Lorentz theory than for the Kramers-Kronig techniques. This difference in $N(\lambda)_l$ beyond 25 μm is attributed to the assumption that $R(\lambda) = R(32.8\ \mu m)$ for the Kramers-Kronig technique in the spectral region $32.8 \leq \lambda \leq \infty$ μm. The values of $N(\lambda)_l$ in the region beyond 25 μm as computed from the Lorentz theory are therefore preferred over those obtained from the Kramers-Kronig technique.

The regions of anomalous dispersion shown in the spectrum for $n(\lambda)_l$ and strong absorption shown in the spectrum of $k(\lambda)_l$, centered at wavelengths 7.00, 11.4, and 14.05 in Figs. 4 and 5, are characteristic of the ordinary and extraordinary rays in birefringent calcite ($CaCO_3$).

**Table I. Lorentz Parameters for Near-Normal Incidence Absolute Reflectance $R(\lambda)_l$ of Limestone**

| $j$ | $\lambda_j$(μm) | $\nu_j$(cm$^{-1}$) | $\rho_j$ | $\gamma_j$ |
|---|---|---|---|---|
| 1 | 6.9 | 1449 | 0.032 | 0.0521 |
| 2 | 11.4 | 877 | 0.0055 | 0.0188 |
| 3 | 14.0 | 714 | 0.0054 | 0.0070 |
| 4 | 33.0 | 303 | 0.140 | 0.0620 |
| $\epsilon_\infty = 2.38$ | | | | |

## V. Conclusions

We determined $N(\lambda)_l$ for limestone throughout the 0.2–32.8-$\mu$m spectral region by a combination of Kramers-Kronig techniques and Lorentz dispersion theory applied to near-normal incidence reflectance spectra. The values of $N(\lambda)_l$ obtained are applicable to data analysis in remote sensing experiments and to Mie computations of the attenuation of ir radiation in dust clouds composed of small limestone particles. However, one question remains open at this point, and that is our assumption that limestone can be treated optically as a homogeneous isotropic material. This question can only be answered by use of the Fresnel equations to compute the reflectance spectra of limestone at oblique angles of incidence and then comparison of the calculated spectra with reflectance spectra measured at the same angles of incidence. We shall seek an answer to this question in the near future.

A few copies of a tabulation of $N(\lambda)$ obtained by use of Kramers-Kronig analysis are available and may be acquired by writing to the authors.

This work was supported in part by the U.S. Army Research Office.

## References

1. G. M. Hale, W. E. Holland, and M. R. Querry, Appl. Opt. **12**, 48 (1973).
2. M. R. Querry, R. C. Waring, W. E. Holland, L. M. Earls, M. D. Herrman, W. P. Nijm, and G. M. Hale, J. Opt. Soc. Am. **64**, 39 (1974).
3. J. R. Aronson and P. F. Strong, Appl. Opt. **14**, 2914 (1975).
4. J. B. Pollack, O. B. Toon, and B. N. Khare, Icarus **19**, 372 (1973).
5. W. G. Spitzer and D. A. Kleinman, Phys. Rev. **121**, 1324 (1961).
6. W. E. Holland, M. R. Querry, and R. M. Coveney, Jr., "Measurements of spectral reflectance and optical constants of selected rock samples of application to remote sensing of soil moisture," Completion Report, U.S. Dept. of Commerce grant 04-4-158-27, available from National Technical Information Service, Springfield, Va. 22151.
7. H. P. Ross, J. E. M. Adler, and G. R. Hunt, Icarus **11**, 46 (1969).
8. R. D. Watson, Remote Sensing Environ. **2**, 95 (1972).
9. G. R. Hunt and J. W. Salisbury, Mod. Geol. **1**, 283 (1970). G. R. Hunt, J. W. Salisbury, and C. J. Lenhoff, Mod. Geol. **2**, 195 (1971).
10. J. M. Hunt, M. P. Wisherd, and L. C. Bonham, Anal. Chem. **22**, 1478 (1950).
11. W. B. Howe and J. W. Koenig, Mo. Geol. Surv. Water Resour. **40**, 2nd Ser., 100 (1961).
12. G. M. Hale and M. R. Querry, Appl. Opt. **12**, 555 (1973).